A Comparative Analysis of the Photon Beam Percentage Depth Dose in an Elekta Linear Accelerator at a Comprehensive Cancer Center

Rajan Prajapati[1*], Junaid Abdul Salam[1], Abish Adhikari[1], Gerim Prasai[1], Subhas Pandit[2], Simit Sapkota[2], Anjani Kumar Jha[2]

[1] Department of Radiation Oncology, Kathmandu Cancer Center, Tathali, Bhaktapur, Nepal
[2] Department of Clinical Oncology, Kathmandu Cancer Center, Tathali, Bhaktapur, Nepal

***CORRESPONDING AUTHOR:**

Rajan Prajapati
Email: rajanprajapati1617@gmail.com

ISSN : 2382-5359(Online), 1994-1412(Print)

DOI:
https://doi.org/10.3126/njst.v22i2.100112

Date of Submission: 13 Apr, 2026

Date of Acceptance: 29 May, 2026

ABSTRACT

This study aims to verify the photon beam energy characteristics of an Elekta Synergy Platform LINAC at Kathmandu Cancer Center, Tathali Nala road by comparing measured PDD data with established British Journal of Radiology (BJR) Supplement 25 and other published literature. PDD measurements were performed for photon energies of 4 MV, 6 MV, and 15 MV using seven different field sizes. All measurements were taken under consistent environmental and setup conditions, including identical pressure, temperature, incremental depth steps, geometry, chamber voltage, and polarity.

For the reference 10 × 10 cm² field size, the measured maximum depth doses (d_{max}) were found to be 1.18 cm, 1.58 cm, and 2.68 cm for 4 MV, 6 MV, and 15 MV photon beams, respectively. The corresponding PDD values at 10 cm depth (d_{10}) were 62.2% for 4 MV, 66.1% for 6 MV, and 74.9% for 15 MV photon energies.

The measured values for 4, 6, and 15 MV photon beams fell within acceptable tolerance limits. The resulting PDD curves demonstrated strong agreement with the reference data in BJR-25 and other published studies, thereby confirming the consistency of beam quality of the Elekta Synergy Platform LINAC.

Keywords: Linear accelerator, Photon beam, Radiotherapy, percentage depth dose (PDD).

1. INTRODUCTION

A linear accelerator (LINAC) is an advanced device used in radiation therapy for cancer treatment, capable of producing high-energy X-ray (photon) or electron beams that precisely target tumors while reducing radiation exposure to surrounding healthy tissues (Corradini et al., 2019). Photon beams are the most used modality in radiotherapy, and a thorough understanding of their dosimetric properties and is essential for accurate and effective treatment planning.

The quality of a photon beam is chiefly determined by its penetrating ability, which is related to its mean photon energy. This characteristic is effectively assessed by the Percentage Depth Dose (PDD) in water (Kato et al., 2004). PDD is therefore a fundamental parameter in radiation dose calculations, ensuring that the prescribed dose is accurately delivered to the tumor (Memon et al., 2015). As direct measurement of dose distribution within a patient is not feasible, PDDs are measured in a homogeneous water phantom that closely mimics human tissue (Ali et al., 2023). These measurements are subsequently incorporated into the treatment planning system (TPS) to determine the absorbed dose for clinical radiotherapy applications (Khan & Gibbons, 2014; Xhafa et al., 2014).

The absorbed dose distribution within the patient depends on several influencing factors, including field size, beam energy, source-to-surface distance (SSD), depth, angle of beam incidence, and beam-modifying devices (Bilge et al., 2010). High-precision dose delivery is vital, as even slight inaccuracies can significantly impact treatment outcomes. Research has shown that a 5% deviation in absorbed dose may result in a 10–20% change in tumor control probability and a 20–30% increase in normal tissue complications (Brahme, 1984). Similarly, dose deviations of 10–15% variation can potentially reduce the probability of cure while increasing irreversible damage by two to three times. Therefore, radiotherapy requires strict adherence to dose accuracy within ±5% of the prescribed dose to safeguard surrounding organs and critical structures (Omer, 2015).

Accurate acquisition of beam data is essential to ensure reliable treatment delivery, as any discrepancies may affect every patient treated with the system (Knutson et al., 2018). In this context, PDD measurements play a crucial role in providing precise information on dose deposition at various depths within tissues, thereby supporting optimal treatment planning and clinical outcomes (Mihailidis, 2011).

Therefore, this study aims to measure and validate PDDs across different field sizes and depths, comparing the results with established reference data to ensure the quality assurance and performance reliability of the Elekta Synergy Platform LINAC at Kathmandu Cancer Center, Nepal.

2. MATERIALS AND METHODS

2.1 Linear Accelerator and Photon Beam Specifications

This study was conducted using an Elekta Synergy Platform linear accelerator, commissioned in 2016, capable of delivering dual-energy photon beams of 4 MV, 6 MV, and 15 MV, as well as multiple electron energies ranging from 4 MeV to 15 MeV. For the purposes of this study, PDD measurements were performed specifically for the photon beams of 4 MV, 6 MV, and 15 MV.

2.2 Measurement Setup

2.2.1 Phantom and Chamber Configuration

PDD measurements were carried out using a 3D water phantom (The Ecophan Water Phantom, IBA). A CC13 ionization chamber (SN 14089) was used as the field chamber and positioned along the central axis inside the water phantom. A second CC13 ionization chamber (SN 14077) served as the reference chamber and was placed just above the water surface outside the primary beam to continuously correct for variations in beam output. All measurements were managed using IBA myQA Accept software version 2016-001 (8.0.1.0) in accordance with the IAEA TRS-398 dosimetry protocol (2004).

2.2.2 Chamber Positioning and Effective Point of Measurement

The water phantom was leveled using a spirit level, and the source-to-surface distance (SSD) was maintained at 100 cm. The field chamber was initially aligned with the water surface to define zero depth. To account for the Effective Point of Measurement (EPOM), the field chamber was shifted downstream by half of its internal radius (0.5r) of the CC13 ionization chamber SN 14089, as recommended by the IAEA (Musolino, 2001). After adjustment, the zero depth was re-established, ensuring accurate measurement along the central axis.

2.3 Percentage Depth Dose (PDD)

The Percentage Depth Dose (PDD) is defined as the ratio of the absorbed dose at a specific depth along the central axis of the beam to the dose at a reference depth, expressed as a percentage. Mathematically, it is represented as:

$$PDD = D_P / D_Q * 100\%$$

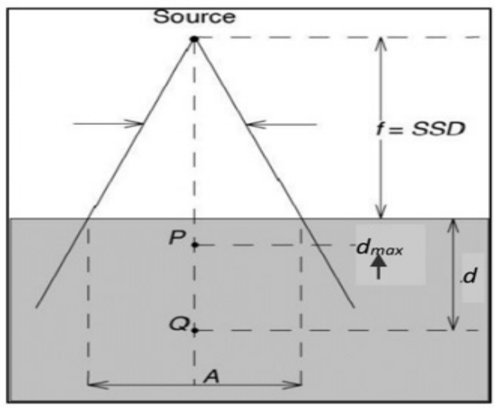

Fig 1: The Setup for PDD measurement (IAEA TRS 398 2004).

where represents the absorbed dose at depth Q, and represents the absorbed dose at the reference depth, P. Measurement of the PDD along the central axis is a key component of LINAC commissioning, as it provides essential information for accurate dose calculations in treatment planning (Khan & Gibbons, 2014).

2.4 Measurement Procedure

During the experiment, the field chamber was mounted inside the water phantom along the central beam axis, while the reference chamber monitored output stability. Continuous scanning was performed from a depth of 35 cm up to the water surface (0 mm) to minimize disturbances caused by water movement. The scanning and data acquisition processes were fully automated and controlled by the myQA Accept software (Mani et al., 2018).

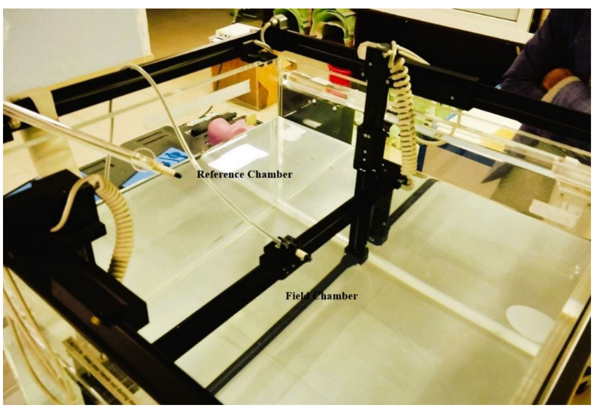

Fig 2: Phantom setup for PDDs measurements

2.5 Field Sizes and Beam Configuration

PDDs were measured for seven square field sizes: 5 × 5, 7 × 7, 10 × 10, 15 × 15, 20 × 20, 30 × 30, and 40 × 40 cm². The Field sizes were defined using the collimator jaws rather than multileaf collimators (MLCs) to avoid dosimetric uncertainties caused by leaf transmission or interleaf gaps (Rahman et al., 2021).

2.6 Data Processing

The measured PDD curves were smoothed using the myQA Accept software. Further analysis, graph plotting, and final presentation of the PDD curves were performed using Microsoft Excel (Microsoft Office Professional 2016).

3. RESULTS

3.1 PDD Curves for Different Field Sizes

The percentage depth dose (PDD) curves for photon energies of 4 MV, 6 MV, and 15 MV across various field sizes normalized d_{max} are presented in Figures 3, 4, and 5, respectively. For all beam energies, the PDD initially increases rapidly in the buildup region, reaches a maximum at d_{max}, and then gradually decreases with depth due to photon attenuation and scattering. The magnitude of the PDD and the depth of the maximum dose are influenced by both photon energy and field size. Higher photon energies exhibit greater penetration, resulting in higher PDD values at the same depth compared to lower-energy beams.

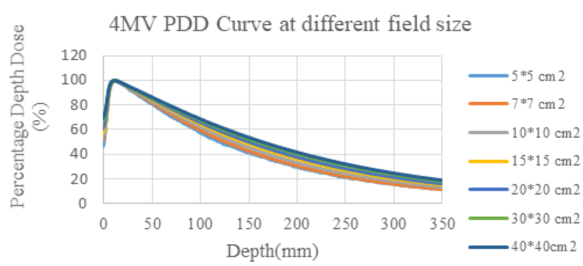

Fig 3: 4MV PDDs Curve at different field sizes

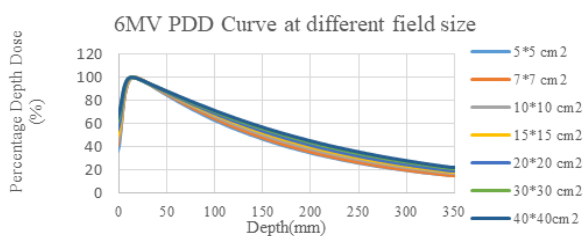

Fig 4: 6MV PDDs Curve at different field sizes.

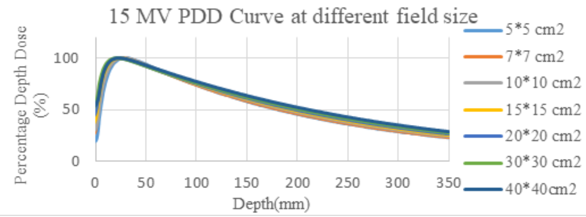

***Fig 5:** 15MV PDDs Curve at different field sizes*

3.2 Surface Dose, Depth of Maximum Dose, and Depth of 50% Dose

The measured surface dose (d_s), depth of maximum dose (d_{max}), depth at 10 cm (D_{10}), and depth of 50% dose (d_{50}) for different field sizes and photon energies are summarized in Table 1. For the standard 10 × 10 cm² field, the surface doses were 57.2%, 52.6%, and 32.8% for 4 MV, 6 MV, and 15 MV beams, respectively. The corresponding depths of maximum dose were 1.18 cm, 1.58 cm, and 2.68 cm, indicating that the point of peak dose shifts deeper as photon energy increases.

The average dose increase per centimeter up to d_{max} was 42.37% for 4 MV, 31.65% for 6 MV, and 18.66% for 15 MV beams. The percentage increase in dose per centimeter in the build-up region decreased with increasing photon energy. The 4 MV beam exhibited the steepest dose build-up (42.37% per cm), followed by 6 MV (31.65% per cm) and 15 MV (18.66% per cm). This trend reflects the deeper d_{max} and improved skin-sparing characteristics of higher-energy photon beams (Podgorsak, 2005). Conversely, the dose fall-off from d_{max} to d_{50} decreased with increasing photon energy, with measured average reductions of 4.05%, 3.72%, and 3.081% per centimeter for 4 MV, 6 MV, and 15 MV beams, respectively. Smaller field sizes exhibited a slightly higher dose fall-off, likely due to reduced contribution from overlapping scatter regions.

3.3 Standard Field Size PDD Profiles

Figure 6 presents the PDD curves for a 10 × 10 cm² reference field at Photon energies of 4 MV, 6 MV, and 15 MV. The curves demonstrate the rapid buildup of dose in the first few millimeters, followed by a gradual decrease after reaching d_{max}. As expected, the depth of maximum dose increases with photon energy, while the surface dose decreases. These trends are consistent with the physical behavior of photon beams, where higher-energy photon beams penetrate deeper before depositing the maximum dose.

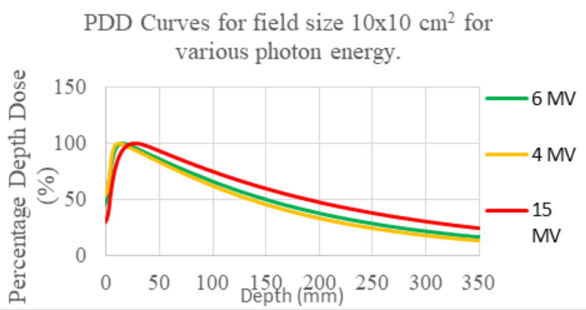

***Fig 6:** PDD curves for a 10 × 10 cm² field size at different photon beam energies*

3.4 Observations across field sizes

As the field size increases from 5 × 5 cm² to 40 × 40 cm², the surface dose and D_{10} values increase for all photon energies, reflecting increased scatter contributions from larger fields. The depth of maximum dose, however, shows a slight decrease with larger fields at lower photon energies, while remaining relatively stable at higher photon energies. These results align with expected dosimetric behavior and provide essential reference data for treatment planning and LINAC commissioning (Khan & Gibbons, 2014; Podgorsak, 2005).

Table 1: Surface dose (ds), depth of maximum dose (d max), and depth of 50% dose (d_{50}) for different field sizes of 4MV, 6 MV, and 15 MV photon beams.

Field Size (cm^2)	Surface Dose d_s (%)			Depth of max. dose dmax(cm)			PDD at 10 cm			Depth at which 50% dose(d_{50}) in cm.		
	4MV	6 MV	15 MV	4MV	6MV	15MV	4MV	6MV	15MV	4 MV	6 MV	15MV
5*5	51.3	45.6	20.9	1.18	1.57	3.18	57.4	62.7	74.2	12.07	13.77	18.22
7*7	55.6	50.5	31.9	1.18	1.58	2.68	60.0	64.5	74.0	12.76	14.33	18.32
10*10	57.2	52.6	31.9	1.18	1.58	2.68	62.2	66.1	74.9	13.51	15.02	18.91
15*15	60.7	57.7	42.7	1.18	1.38	2.38	64.5	67.9	75.1	14.42	15.88	19.40
20*20	64.1	62.4	48.9	1.18	1.38	2.28	66.0	68.9	75.4	15.05	16.43	19.80
30*30	69.6	69.3	56.2	1.18	1.38	2.08	67.6	70.4	76.0	15.89	17.29	20.40
40*40	72.4	71.6	55.0	1.07	1.37	2.38	68.7	71.2	77.2	16.44	17.84	21.07

4. DISCUSSION

The observed percentage depth-dose (PDD) behavior in this study is consistent with the physical principles of photon interactions in tissue-equivalent media. Beyond the depth of maximum dose (d_{max}), PDD decreases with increasing depth due to photon attenuation, scattering, and the inverse square law. Conversely, higher-energy photon beams exhibit greater penetration, resulting in higher PDD values at a given depth compared to lower-energy beams (Khan & Gibbons, 2014). In the buildup region, PDD increases with depth due to the generation of secondary electrons, which deposit their energy over a short distance downstream of their origin before being fully stopped.

The dependence of PDD on field size is influenced by photon energy. For a lower-energy Photon beam, increasing the field size enhances the contribution of scattered radiation, resulting in higher PDD values. However, as photon energy increases, the probability of scattering decreases, and photons tend to scatter more in the forward direction. Consequently, the effect of field size on PDD diminishes for higher-energy beams (Rahman et al., 2021; Podgorsak, 2005; Roy et al., 2021).

4.1 Comparison with BJR-25 and Published Data

The measured PDD values for photon beam of 4 MV, 6 MV, and 15 MV with a reference field size of 10 × 10 cm^2 were plotted, normalized the measured dose value to 100% at dmax and compared to the reference data from BJR Supplement 25. Figures 7 to 9 illustrate the PDD curves for the three photon energies, demonstrating excellent agreement between the measured data and BJR-25 reference values (Bewley, 1983). Table 2 further confirms the consistency of key dosimetric parameters, including the dose at 10 cm depth (D_{10}), depth of 80% dose (D_{80}), depth of maximum dose (d_{max}), and the dose fall-off from d_{max} to D_{50}. The measured values align closely with BJR-25 and other published datasets, validating the commissioning data for the Elekta Synergy LINAC.

For 4 MV beam, the measured d_{max} was 1.18 cm, d_{10} was 62.2%, and d_{80} was 5.75 cm, closely matching BJR-25 values of 1.0 cm, 63.0%, and 5.9 cm, respectively. Similarly, the 6 MV beam measurements yielded a d_{max} of 1.58 cm, d_{10} of 66.1%, and d_{80} of 6.42 cm, closely matching BJR-25 values of 1.5 cm, 67.5.0%, and 6.7 cm, respectively. Also, for the 15 MV beam, the measured d_{max} was at 2.68 cm, d_{10} at 74.9%, and d_{80} at 8.52 cm, closely matching BJR- 25 values of 2.9 cm, d_{10} was 77%, and d_{80} was 9.1 cm, respectively. The Commissioning data show small deviations from BJR-25 values for d_{10}, d_{80}, d_{max} and dose fall off, which are expected due to the machine-specific nature of measured data. BJR-25 represents average reference beam data, whereas commissioning measurements reflects the unique beam characteristics of the Linac, including target design, flattering filter geometry, and head scatter (Khan & Gibbons, 2014; Podgorsak, 2005). The observed difference, typically within 1-3% for d_{10} and within a few millimeters for depth parameters, is consistent with published studies and lies within acceptable dosimetric tolerances for clinical use (IAEA TRS 398 2004; Buzdar et al., 2009; Mia et al., 2019). The dose fall-off per centimeter from d_{max} to d_{50} also matches reference values, further confirming the accuracy of the measured PDD curves.

Table 2: Comparison of measured data with BJR-25 and other published studies for a reference field size of 10 × 10 cm².

Energy	Observation	d_{10} (%)	d_{80} (cm)	d_{max} (cm)	Fall of dose d_{max} to d_{50}(%/cm)
4MV	BJR 25	63.0	5.9	1.0	3.906
	Commissioning Data	62.2	5.75	1.18	4.055
	Buzdar et al. 2009	-	-	1.0	3.88
	Mia et al. 2019	-	-	-	-
6MV	BJR 25	67.5	6.7	1.5	3.546
	Commissioning Data	66.1	6.42	1.58	3.720
	Buzdar et al. 2009	-	-	1.5	3.55
	Mia et al. 2019	66.8	-	1.58	3.72
15MV	BJR 25	77.0	9.1	2.9	2.934
	Commissioning Data	74.9	8.52	2.68	3.081
	Buzdar et al. 2009	-	-	2.9	2.92
	Mia et al. 2019	76.8	-	2.79	2.96

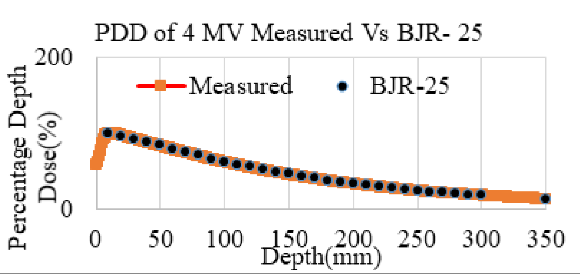

Fig 7: PDD curve for a 10 × 10 cm² field size using a 4 MV photon beam

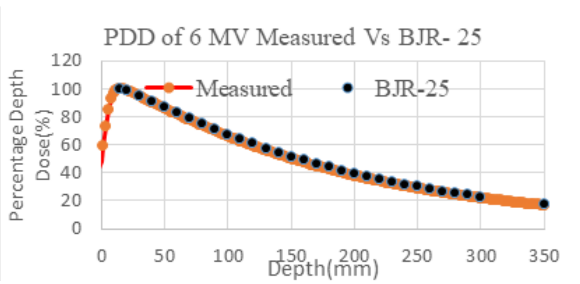

Fig 8: PDD curve for a 10 × 10 cm² field size using a 6 MV photon beam

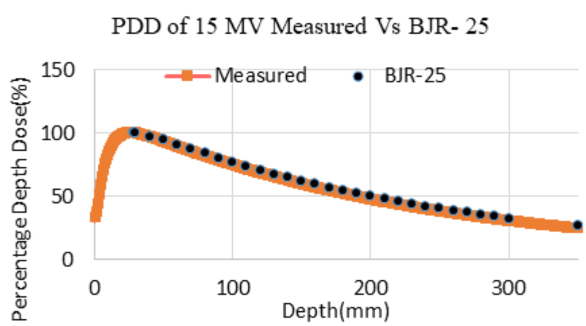

Fig 9: PDD curve for a 10 × 10 cm² field size using a 15 MV photon beam

4.2 Compliance with International Protocols

For low-energy photon beams (<10 MV), the expected PDD at a 10 cm depth should be up to 75%. For higher-energy beams, it can reach up to 89% (Almond et al., 1999; Shimozato et al., 2017). In this study, the PDD values at 10 cm depth were 62.2%, 66.1%, and 74.9% for 4 MV, 6 MV, and 15 MV beams, respectively. These results are well within the recommended tolerance limits, indicating that the Elekta Synergy LINAC meets the dosimetric standards specified in the AAPM TG-51 protocol (Kragl et al., 2009; Beyer, 2013).

5. CONCLUSION

Accurate knowledge of a linear accelerator's percentage depth dose (PDD) is essential for effective radiotherapy treatment planning, so that the prescribed dose is delivered to the tumor while minimizing exposure to surrounding healthy tissues. In this study, PDD values increase with photon beam energy due to greater penetration and also rise with increasing field size. Conversely, the depth of maximum dose (d_{max}) increases with higher beam energy but slightly decreases with larger field sizes. The measured PDDs showed excellent agreement with reference data from BJR-25 and other published studies across multiple depths and field sizes, confirming the reliability of the Elekta Synergy LINAC. These results reinforce accurate dose calculation, provide essential guidance for optimizing treatment planning, and contribute to enhanced precision and improved clinical outcomes in radiotherapy.

REFERENCES

Ali, J., Sohail, M., Samad, A., Ahmad, I., Soomro, H., Biradar, G., Naz, I., & Tariq, I. (2023). Comparison of percentage depth doses with the published data for Co-60 radiotherapy machine at a regional cancer hospital. *Journal of Physics and Its Applications, 6*(1), 24–30.

Almond, P. R., Biggs, P. J., Coursey, B. M., Hanson, W. F., Huq, M. S., Nath, R., & Rogers, D. W. (1999). AAPM's TG-51 protocol for clinical reference dosimetry of high-energy photon and electron beams. *Medical Physics, 26*(9), 1847–1870.
DOI: 10.1118/1.598691
PMID: 10505874

Bewley, D. K. (1983). Central axis depth dose data for use in radiotherapy. *Br. J. Radiol. Suppl., 17*, 1–47.

Beyer, G. P. (2013). Commissioning measurements for photon beam data on three TrueBeam linear accelerators, and comparison with Trilogy and Clinac 2100 linear accelerators. *Journal of Applied Clinical Medical Physics, 14*(1), 273–288.
DOI: 10.1120/jacmp.v14i1.4077
PMID: 23318395 PMCID: PMC5714054

Bilge, H., Ozbek, N., Okutan, M., Cakir, A., & Acar, H. (2010). Surface dose and build-up region measurements with wedge filters for 6 and 18 MV photon beams. *Japanese Journal of Radiology, 28*(2), 110–116.
DOI: 10.1007/s11604-009-0393-5
PMID: 20182845

Brahme, A. (1984). Dosimetric precision requirements in radiation therapy. *Acta Radiologica: Oncology, 23*(5), 379–391.
DOI: 10.3109/02841868409136037
PMID: 6095609

Buzdar, S. A., Rao, M. A., & Nazir, A. (2009). An analysis of depth dose characteristics of photon in water. *Journal of Ayub Medical College Abbottabad, 21*(4), 41–45.

Corradini, S., Alongi, F., Andratschke, N., Belka, C., Boldrini, L., Cellini, F., Debus, J., Guckenberger, M., Hörner-Rieber, J., Lagerwaard, F. J., & Mazzola, R. (2019). MR-guidance in clinical reality: Current treatment challenges and future perspectives. *Radiation Oncology, 14*(1), 92.
DOI: 10.1186/s13014-019-1308-y
PMID: 31167658 PMCID: PMC6551911

International Atomic Energy Agency. (2004). *Absorbed dose determination in external beam radiotherapy: An international code of practice for dosimetry based on standards of absorbed dose to water* (Technical Report Series No. 398). IAEA.

Jordan, T. J. (1996). Section 5. Megavoltage x-ray beams: 2–50 MV. *Br. J. Radiol. Suppl., 25*.

Kato, H., Fujii, S., & Suzuki, S. (2004). Method of calculating percentage depth dose for diagnostic X-rays. *Nihon Hoshasen Gijutsu Gakkai Zasshi, 60*(8), 1107–1115.
DOI: 10.6009/jjrt.KJ00000922571
PMID: 15389168

Khan, F. M., & Gibbons, J. P. (2014). *Khan's the physics of radiation therapy*. Lippincott Williams & Wilkins.

Knutson, N. C., Schmidt, M. C., Belley, M. D., Nguyen, N., Price, M., Mutic, S., Sajo, E., & Li, H. H. (2018). Equivalency of beam scan data collection using a 1D tank and automated couch movements to traditional 3D tank measurements. *Journal of Applied Clinical Medical Physics, 19*(6), 60–67.
DOI: 10.1002/acm2.12444 PMID: 30188009 PMCID: PMC6236829

Kragl, G., af Wetterstedt, S., Knäusl, B., Lind, M., McCavana, P., Knöös, T., McClean, B., & Georg, D. (2009). Dosimetric characteristics of 6 and 10 MV unflattened photon beams. *Radiotherapy and Oncology, 93*(1), 141–146.
DOI: 10.1016/j.radonc.2009.06.008
PMID: 19592123

Mani, K. R., Bhuiyan, M. A., Rahman, M. S., & Islam,

S. A. (2018). Open beam dosimetric characteristics of TrueBeam medical linear accelerator with flattening filter (WFF) and flattening filter free (FFF) beam. *Polish Journal of Medical Physics and Engineering, 24*(2), 79–89.
DOI: 10.2478/pjmpe-2018-0011

Memon, S. A., Laghari, N. A., Mangi, F. H., Ahmad, F., Hussain, M. M., Palijo, S., Jhatyal, N., & Adeel, A. (2015). Analysis and verification of percent depth dose and tissue maximum ratio for Co-60 gamma ray beam. *World Applied Sciences Journal, 33*(1), 109–113.

Mia, M. A., Rahman, M. S., Purohit, S., Kabir, S. M., & Meaze, A. K. (2019). Analysis of percentage depth dose for 6 and 15 MV photon energies of medical linear accelerator with CC13 ionization chamber. *Nuclear Science and Applications, 28*(1&2).

Mihailidis, D. (2011). *The physics & technology of radiation therapy*.
DOI: 10.1118/1.3594546

Musolino, S. V. (2001). Absorbed dose determination in external beam radiotherapy: An international code of practice for dosimetry based on standards of absorbed dose to water; Technical Reports Series No. 398.
DOI: 10.1097/00004032-200111000-00017

Omer, M. A. (2015). Partial quality assessment of ^{60}Co-teletherapy machine performance. *Open Journal of Radiology, 5*(4), 235.
DOI: 10.4236/ojrad.2015.54032

Podgorsak, E. B. (2005). Treatment machines for external beam radiotherapy. In *IAEA radiation oncology physics: A handbook for teachers and students*. International Atomic Energy Agency.

Rahman, M., Shamsuzzaman, M., Sarker, M., Jobber, A., Mia, M., Bairagi, A. K., Ahmed, M., Reza, S., Malik, S. R., Bhuiyan, M. M., & Khan, A. H. (2021). Dosimetric characterization of medical linear accelerator photon and electron beams for the treatment accuracy of cancer patients. *World Journal of Advanced Engineering Technology and Sciences, 3*(1), 41–59.
DOI: 10.30574/wjaets.2021.3.1.0046

Roy, S. K., Das, P. K., Khatun, R., Rahman, M. A., Akter, S., Kumar, T., & Ahasan, M. M. (2021). Dosimetric characteristics of 6 MV medical linac at BAEC. *International Journal of Medical Physics, Clinical Engineering and Radiation Oncology, 10*(1), 38.
DOI: 10.4236/ijmpcero.2021.101004

Shimozato, T., Aoyama, Y., Matsunaga, T., & Tabushi, K. (2017). Beam characterization of 10-MV photon beam from medical linear accelerator without flattening filter. *Journal of Medical Physics, 42*(2), 65–71.
DOI: 10.4103/jmp.jmp_71_16
PMID: 28706351 PMCID: PMC5496272

Xhafa, B., Mulaj, T., Hodolli, G., & Nafezi, G. (2014). Dose distribution of photon beam by Siemens linear accelerator. *International Journal of Medical Physics, Clinical Engineering and Radiation Oncology.*
DOI: 10.4236/ijmpcero.2014.31011